Including frequency-dependent attenuation for the deconvolution of ultrasonic signals

Ewen Carcreff[1,2], Sébastien Bourguignon[1], Jérôme Idier[1], Laurent Simon[2], Aroune Duclos[2]

[1] LUNAM Université / IRCCyN lab, 1 rue de la Noë, 44321 Nantes, France
[2] LUNAM Université / LAUM lab, avenue Olivier Messiaen, 72085, Le Mans, France

Abstract

Ultrasonic non-destructive testing (NDT) is a standard process for detecting flaws or discontinuities in industrial parts. A pulse is emitted by an ultrasonic transducer through a material, and a reflected wave is produced at each impedance change. In many cases, echoes can overlap in the received signal and deconvolution can be applied to perform echo separation and to enhance the resolution. Common deconvolution techniques assume that the shape of the echoes is invariant to the propagation distance. This can cause poor performances with materials such as plastics or composites, in particular because acoustic propagation suffers from frequency-dependent attenuation. In geophysics, biomedical imaging or NDT, various frequency-dependent attenuation models have been proposed under different formulations. This communication compares the related possible constructions in order to account for attenuation in deconvolution methods. Especially, we introduce a discrete model for the data, that includes an attenuation matrix in the standard convolution model. Experimental data acquired from Plexiglas plates show that, for this material, attenuation varies roughly linearly with frequency, leading to the identification of a unique parameter. Finally, we show that such an advanced model manages a better fitting of the data, and promises improvement for the deconvolution of complex ultrasonic data.

INTRODUCTION

In the context of non-destructive testing (NDT) by ultrasound, a pulse is emitted by an ultrasonic transducer through a material, and, in a pulse-echo configuration, a reflected wave is produced at each impedance change. The analysis of the times of flight of the echoes received by the transducer allows for the characterization of the interfaces, and possible flaws, in the inspected object. When the reflectors are close, the echoes overlap and the analysis of the signal becomes a hard task. This is for example more pronounced for composite materials where the layers are very close. The problem is commonly solved by performing deconvolution, and many investigations have been carried out in this field [1, 2]. Those techniques usually consider that the received echoes are delayed and scaled replicas of an *a priori* known reference waveform. It is actually an assumption of non-attenuative medium, that is imprecise for certain types of materials (plastics, composites, *etc.*). The deconvolution may have poor performances for those materials because the shape of the echoes is changing with propagation distance, due to frequency-dependent attenuation [3]. The latter is indeed a function of frequency and distance of propagation [4]. In the biomedical imaging community [4, 5, 6], the attenuation is usually formulated by a log-linear frequency dependence with a unique parameter α_0 for a material. This formulation has an equivalent in the geophysics field, known as the constant-Q model [7, 8] and implying a quality factor Q, inversely proportional to α_0.

The contribution of this communication is to include the frequency-dependent attenuation in the considered signal model. In order to achieve this, we consider a discrete convolution model mainly employed in deconvolution methods. The purpose is then to introduce an attenuation matrix that describes the attenuation, as a function of the propagation distance, in a discrete manner. Olofsson *et al.* use this model for the deconvolution of signals acquired from a composite [3], and lead to satisfactory results. They use a simple attenuation function based on a first order discrete filter. We propose to generalize this construction to other attenuation models, and to compare the related models from NDT, geophysics and biomedical imaging communities.

The rest of the paper is organized as follows. In section 2, we present the frequency-dependent attenuation model commonly employed in the literature. Then, the discrete model of convolution including the attenuation matrix is introduced in section 3. In section 4, experimental data allows us

to identify the attenuation parameter and to check the discrete model validity. Finally, conclusions and perspectives are given in section 5.

FREQUENCY-DEPENDENT ATTENUATION MODEL

Signal model of an ultrasonic measurement

In this section, we focus on the signal formation of an ultrasonic measurement. The configuration can either be a transmit/receive (T/R) mode or a pulse/echo (P/E) mode (see figure 1 for a visual description of those modes). In the frequency domain, the output signal $Y(f)$ received by the transducer depends on the electrical excitation $U(f)$ through a set of transfer functions. Therefore, the time domain signal $y(t)$ is simply the convolution of the impulse responses, that are the inverse Fourier transforms of the transfer functions. We consider a single scatterer located at $\boldsymbol{r}$ and defining a propagation path $\boldsymbol{z}$. In T/R mode, $\boldsymbol{z}$ represents the path from the transmitting transducer to the scatterer, and from the scatterer to the receiving transducer. In P/E mode, we have a round-trip, that is the path from the transducer to the reflector and back. The received signal in the frequency domain is then given by [9]:

$$Y(f,\boldsymbol{z}) = U(f)\, H_{ea}(f)\, H_r(f,\boldsymbol{z})\, H_{ae}(f), \tag{1}$$

where $H_{ea}(f)$ and $H_{ae}(f)$ are respectively the electro-acoustical and acousto-electrical transfer functions. For clarity purpose, we consider $U(f)H_{ea}(f)H_{ae}(f)$ as the electrical transfer function $H_e(f)$. The latter corresponds to the reference waveform $h_e(t)$ that is independent of the propagation characteristics. The radiation term $H_r(f,\boldsymbol{z})$ introduced by Stephanishen [10], represents the transfer function of the propagation path. As an example, for a one way path, the radiation function in $\boldsymbol{r}$ is the sum over the radiating surface S of elementary sources ($\boldsymbol{r}_0$ are the positions on S):

$$H_r(f,\boldsymbol{r}) = \int_S \frac{e^{-jk(f)|\boldsymbol{r}-\boldsymbol{r}_0|}}{2\pi|\boldsymbol{r}-\boldsymbol{r}_0|}\,\mathrm{d}S, \tag{2}$$

where $k(f)$ is the wavenumber in the considered material, depending on the wave velocity. In T/R mode, as explained above, the overall radiation function is composed of two different radiation functions, whereas in P/E mode, it is the square of the one-way function. If we consider attenuation, the wavenumber becomes complex: $k(f) = 2\pi f/c_0 + \epsilon(f) - j\alpha(f)$. Note that c_0 is the constant wave velocity. The terms $\alpha(f)$ and $\epsilon(f)$ respectively stand for the amplitude attenuation and the dispersion. Considering the propagation path $\boldsymbol{z}$ is roughly constant for all points $\boldsymbol{r}_0$ of the radiating surface S, the attenuation and dispersion terms can be separated from the constant radiation part. Finally, this leads to the expression of the received signal, for a single reflector whose propagation path is $\boldsymbol{z}$:

$$Y(f,\boldsymbol{z}) = b(|\boldsymbol{z}|)\, H_e(f)\, e^{-\alpha(f)|\boldsymbol{z}|}\, e^{-j\epsilon(f)|\boldsymbol{z}|}\, e^{-j2\pi f|\boldsymbol{z}|/c_0}, \tag{3}$$

with $b(|\boldsymbol{z}|)$ a constant term, depending on the travel distance. The radiation term $e^{-j2\pi f|\boldsymbol{z}|/c_0}$ is a pure delay term, that is equivalent to the impulse response $\delta(t-|\boldsymbol{z}|/c_0)$. The signal received by the transducer is modeled as a set of products in the frequency domain, that is equivalent to a set of convolutions in the time domain.

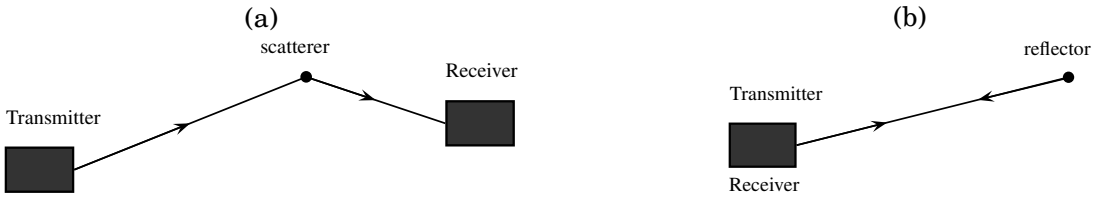

FIGURE 1: (a): Scheme of a Transmit/Receive configuration. (b): Scheme of a Pulse/Echo configuration.

Attenuation model

An acoustic wave propagating in a medium has energy loss due to scattering and absorption. Absorption involves a frequency-dependent attenuation of the ultrasonic waves, that can be generally described by a magnitude and a phase modification $A(f) = e^{-\beta(f) - j\phi(f)}$. In this study, we focus on the amplitude attenuation $e^{-\beta(f)}$ since the phase modification $e^{-j\phi(f)}$, the dispersion, is a more complex phenomenon. In other studies, the dispersion part $\phi(f)$ is usually obtained from the magnitude part $\beta(f)$ by using the Kramers-Kronig relation [11]. In biomedical imaging, the amplitude attenuation is modeled, for a given distance z, as a linear time invariant filter specified in the frequency domain [4]:

$$A(f, z) = e^{-\alpha(f) z}, \tag{4}$$

where $\alpha(f)$ is a function of frequency and z is the propagation distance. We have hence a different attenuation shape for each distance z. The attenuation has a low-pass behavior, meaning that the more z increases, the more severe the filtering. Usually, $\alpha(f)$ is considered as a linear function of frequency such as $\alpha(f) = \alpha_0 |f|$, with α_0 the attenuation parameter in $\mathrm{Np\,MHz^{-1}\,mm^{-1}}$. The previous model is equivalent to the well-known constant-Q model in geophysics, introduced by Kjartansson [7]:

$$A(f, z) = e^{-\frac{\pi |f| z}{Q c_0}}. \tag{5}$$

The quality factor Q is defined as the ratio between the maximum energy stored in the material, and the energy lost during a cycle. It respects $Q = \pi / \alpha_0 c_0$. Q is also inversely proportional to α_0, meaning that when Q is infinite, it corresponds to $\alpha_0 = 0$ (lossless medium). A synthetic example of attenuation with $\alpha_0 = 0.05\,\mathrm{Np\,MHz^{-1}\,mm^{-1}}$ for three distances is shown in figure (2-a). One can notice the augmentation of the filtering effect with respect to the travel distance.

Example: Linear attenuation of a Gaussian waveform

In many acoustic fields (cited in introduction), the reference waveform is modelled as a continuous wave windowed by a Gaussian [4, 6, 12]:

$$h_e(t) = A\, e^{-\frac{(t-t_0)^2}{2\sigma_t^2}} \cos\left(2\pi f_0 (t - t_0) + \phi\right), \tag{6}$$

with A the amplitude, t_0 the time position, σ_t the time standard deviation of the Gaussian, f_0 the center frequency and ϕ the phase. For positive frequencies, the Fourier transform of the Gaussian waveform reads:

$$|H_e(f)| = A'\, e^{-\frac{(f-f_0)^2}{2\sigma_f^2}}, \tag{7}$$

where $A' = A\sigma_t\sqrt{2\pi}$ and $\sigma_f = 1/(2\pi\sigma_t)$. The Fourier transform of the waveform after propagating through a distance z is given by :

$$|Y(f, z)| = A'\, e^{-\frac{(f-f_0)^2}{2\sigma_f^2}}\, e^{-\alpha_0 f z}. \tag{8}$$

It actually leads to an other Gaussian waveform where the standard deviation remains σ_f and f_1 is the new down-shift center frequency such as:

$$f_1 = f_0 - \alpha_0 \sigma_f^2 z. \tag{9}$$

A simulation example is given in figure (2). We plot the normalized magnitude of $Y(f, z)$ for three propagation distances z in figure (2-b). Note that the center frequency decreases as z increases and the bandwidth (related to σ_f) remains constant. In addition, the corresponding waveforms in the time domain are plotted in figure (2-c), showing the width of the waveforms broadens with increased travel distance. One can also notice that the amplitude decrease, both in time and frequency domains, does not appear in the plots because of the normalization. The figure (2-d) shows the center frequency downshift, that is linear with respect to the propagation distance.

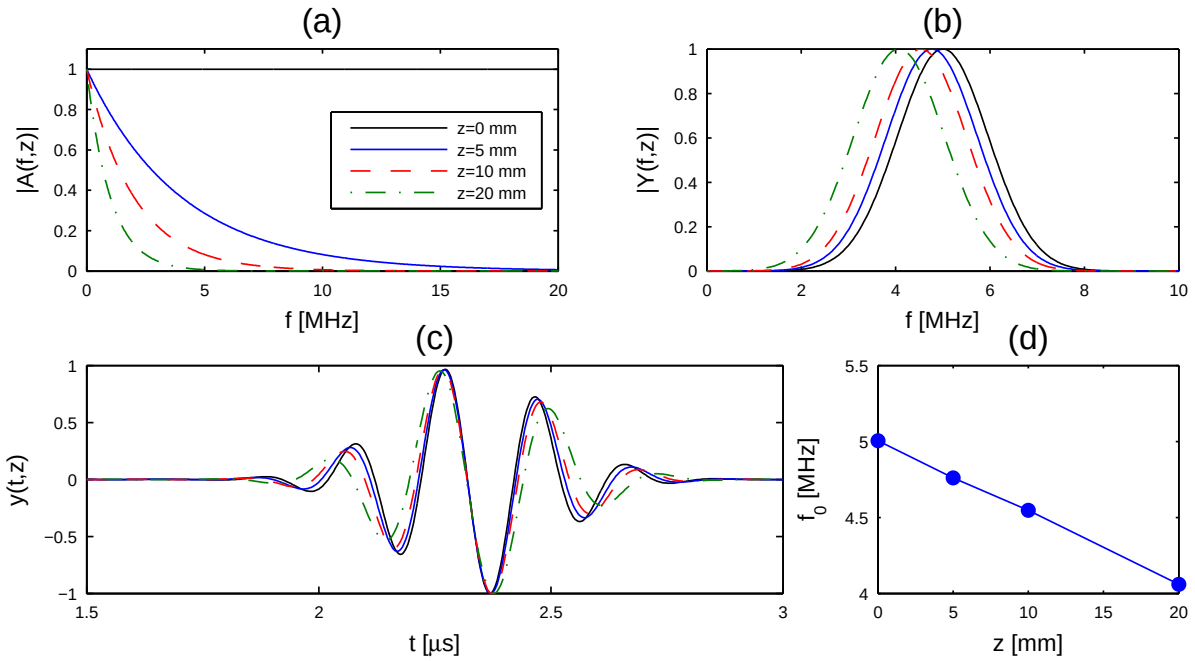

FIGURE 2: Example of attenuation for travel distances z = 5, 10 and 20 mm. The attenuation parameter α_0 is set to $0.05\,\mathrm{Np\,MHz^{-1}\,mm^{-1}}$. (a): Magnitude of the transfer functions $A(f,z)$, (b): normalized magnitude of the received signal $Y(f,z)$, (c): time signals $y(t,z)$, normalized and time aligned, (d): center frequency downshift with respect to the distance.

SIGNAL MODELING AS A NONSTATIONARY DISCRETE CONVOLUTION

Spatial discretization of the attenuation function

We consider a discretization of the travel distance such as $z_n = n\Delta z$, where Δz is the spatial resolution. From equation (4), one can write the discrete attenuation expression:

$$A(f,n) = e^{-\alpha(f)n\Delta z} = \left(e^{-\alpha(f)\Delta z}\right)^n = P(f)^n. \tag{10}$$

For a given n, the latter is therefore equivalent to $n-1$ multiplications of the same kernel $P(f)$. This kernel can actually model any frequency-dependent attenuation that is a linear function of the propagation distance z. It models the transfer function between two distances separated by Δz. In the time domain, equation (10) corresponds to $n-1$ self-convolutions of some time kernel $\rho(t)$, the inverse Fourier Transform of $P(f)$. If T_S is the sampling frequency, let us note ρ_k the discrete kernel such as $\rho_k = \rho(kT_S)$, and $\boldsymbol{\rho}$ the vector collecting the ρ_k. Furthermore, $\boldsymbol{\rho}^{(n)}$ is the notation for $n-1$ self-convolutions of $\boldsymbol{\rho}$. In the following points, we focus on different formulations of the kernel $\boldsymbol{\rho}$:

- Olofsson *et al.* [3] employ the kernel $\boldsymbol{\rho} = [0,\, 1-a,\, a,\, 0]$ where a is close to zero. The choice is motivated by applying a small distortion compared to the Dirac function. Indeed, for $a = 0$, the kernel is the Dirac pulse which implies no frequency-dependent attenuation. This kernel has the transfer function $P(f)$ such as:

$$|P(f)|^2 = 1 - 4a(1-a)\sin^2(\pi f/f_S), \tag{11}$$

  where f_S is the sampling frequency. This filter is not linear with respect to frequency. Its use is hence practical due to the kernel simplicity but has no physical description. The parameter a can be found by fitting a separate echo at a given depth using its Fourier transform.

- The linear attenuation kernel is $P(f) = e^{-\alpha_0 |f| \Delta z}$. $\boldsymbol{\rho}$ can be computed by performing the inverse Fourier transform of $P(f)$. Otherwise, Kak *et al.* [5] identified the impulse response from equation (3):

$$\rho(t) = \frac{1}{\pi} \frac{\alpha_0 \Delta z/2\pi}{(\alpha_0 \Delta z/2\pi)^2 + (t - \Delta z/c_0)^2}. \tag{12}$$

Nonstationary discrete convolution formulation

Let us consider a single scatterer i defining a travel distance z_i such as $z_i = n_i \Delta z$. Since $a(t, z_i)$ is the inverse Fourier transform of the attenuation function $A(f, z_i)$, the time domain signal model for a single scatterer is derived from equation (3):

$$y(t, z_i) = b_i \; h_e(t) * a(t, z_i) * \delta(t - z_i/c_0) = b_i \; h_e(t) * a(t - z_i/c_0, z_i). \tag{13}$$

The term $h_e(t) * a(t - z_i/c_0, z_i)$ stands for the nonstationnary convolution. The signal received by the transducer $y(t)$ is then the sum over all the scatterers: $y(t) = \sum_i y(t, z_i)$. Let us consider the vectors $\boldsymbol{y}$ and $\boldsymbol{h}_e$, collecting the $y(kT_S)$ and the $h_e(kT_S)$ respectively. As $h_e(t)$ is invariant to the propagation distance, a usual formulation considers a convolution matrix $\mathbf{H}$ whose columns are delayed versions of $\boldsymbol{h}_e$ [2, 3]. From the previous part, the attenuative term $a(t - z_i/c_0, z_i)$ actually reads $\rho(t)^{(n_i)}$, that is the impulse response of the attenuation function for $z_i = n_i \Delta z$. Note that generally, the spatial resolution Δz is $c_0 T_S$. From equation (13), one can then write the discrete form:

$$\boldsymbol{y} = \mathbf{H}\left(\sum_i b_i \boldsymbol{\rho}^{(n_i)}\right). \tag{14}$$

Then, we consider a sparse vector $\boldsymbol{x}$ composed of the amplitudes b_i at positions n_i and zeros elsewhere. The model can therefore be formulated as a matrix system:

$$\boldsymbol{y} = \mathbf{H}\,\mathbf{A}\,\boldsymbol{x}. \tag{15}$$

This discrete model has been employed by Olofsson for deconvolution [3], but has been initially introduced in geophysics by Hale [8]. The matrix $\mathbf{A}$ is composed of all the attenuation vectors $\boldsymbol{\rho}^{(n)}$ such as:

$$\mathbf{A} = \left[\boldsymbol{\rho}^{(1)} \; \boldsymbol{\rho}^{(2)} \; \boldsymbol{\rho}^{(3)} \; \cdots\right] = \begin{bmatrix} \rho_0^{(1)} & 0 & 0 & \cdots \\ \rho_1^{(1)} & \rho_1^{(2)} & 0 & \cdots \\ \rho_2^{(1)} & \rho_2^{(2)} & \rho_2^{(3)} & \cdots \\ \vdots & \vdots & \vdots & \ddots \end{bmatrix}. \tag{16}$$

The latter is a lower triangular matrix because the attenuation filters (columns) need to be causal. An illustration of the matrices is shown in figure (3). The waveform is represented by one column of $\mathbf{HA}$, for a traveltime equal to the column time. One can observe the amplitude decrease and the width broadening of the waveform with respect to travel distance. The construction described in this section therefore enables to model a discrete time ultrasonic signal $\boldsymbol{y}$, composed of several echoes and including a frequency-dependent attenuation function. It is important to notice that any attenuation model, that is linear with respect to the propagation distance, can be modeled by a discrete matrix $\mathbf{A}$. In the case of several propagation media, one can build a block diagonal matrix $\mathbf{A}$ composed of the respective media matrices. For example, a water path, which is loss-less, involves the insertion of an identity block matrix $\mathbf{I}$ into $\mathbf{A}$. Nevertheless, this model can not describe multiple reflections, unless a unique material is considered.

The purpose of deconvolution is to estimate the vector $\boldsymbol{x}$ knowing the data $\boldsymbol{y}$. It hence allows us to estimate the b_i and $n_i \Delta z$, which are the amplitudes and positions of the scatterers respectively. The purpose of discretization is to establish a linear relation between those vectors, which simplifies the inversion. Standard deconvolution uses the system $\boldsymbol{y} = \mathbf{H}\boldsymbol{x}$ and takes advantage of the stationary convolution model [1, 2]. An extended deconvolution employs the equation $\boldsymbol{y} = \mathbf{HA}\boldsymbol{x}$, which includes an attenuation matrix [8, 3]. This model is indeed closer to the ultrasonic propagation reality.

Application to experimental data

Identification of the attenuation parameter

In this part, the purpose is to verify the linear attenuation model and possibly to identify the parameter α_0. To do so, we performed pulse-echo measurements in Polymethyl methacrylate

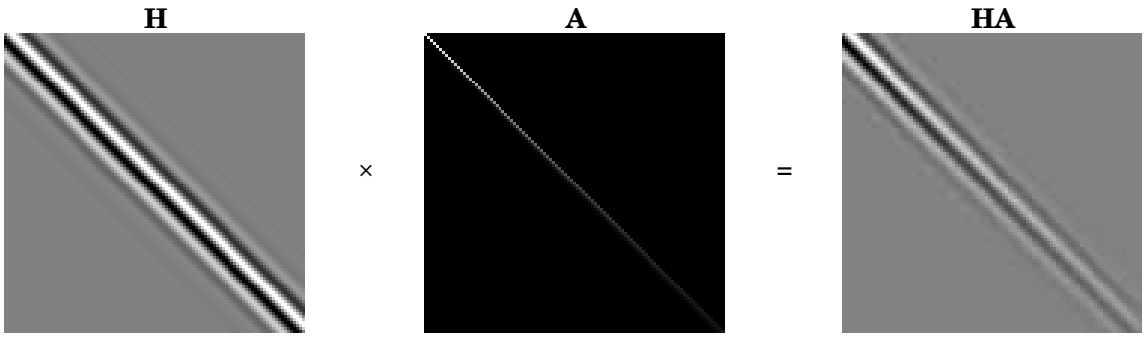

FIGURE 3: An illustration of the matrices involved in equation (15) for a particular attenuation model. **H** is the stationnary convolution matrix whose columns are delayed versions of $\boldsymbol{h}_e$. **A** is the attenuation matrix where each column is the impulse response for a traveltime equal to the column time. **HA** is the resultant nonstationary convolution matrix.

(Plexiglas) plates of different thicknesses, using a non-focused probe of center frequency 2.25 MHz. The measurement apparatus is shown in figure (4-a). The thicknesses of the plates are large enough to have separated echoes from the front wall and the back wall. A signal measured from the 6 mm plate at 2.25 MHz is also shown in figure (4-b). We can note that the attenuation is relatively severe since we can exploit only the three first echoes (the front wall echo and two back wall echoes). Further echoes are blurred into noise. Moreover, we measure the wave velocity in Plexiglas, that is roughly 2802 m/s.

A non-linear least-square curve-fitting allows us to estimate the parameters in the echo model, in Equation (6). This process enables us to find the value of the center frequency for each echo. The results are shown in figure (5-a). One can note that for a given measurement, the center frequency of the echoes is roughly linearly decreasing, that confirms the linear attenuation model proposed above. From Equation (9), one can identify the values of α_0 in $\mathrm{Np\,MHz^{-1}\,m^{-1}}$, which we sum-up in figure (5-b). The processing using other center frequency probes roughly lead to the same results. An average value of the parameter α_0 is $11\,\mathrm{Np\,MHz^{-1}\,m^{-1}}$, equivalent to $0.955\,\mathrm{dB\,MHz^{-1}\,cm^{-1}}$.

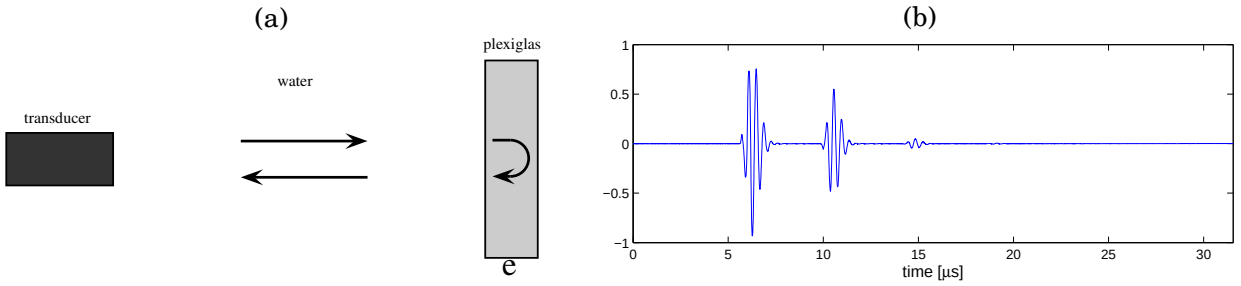

FIGURE 4: (a): Scheme of the pulse-echo measurement in Plexiglas plates. (b): Example of received signal.

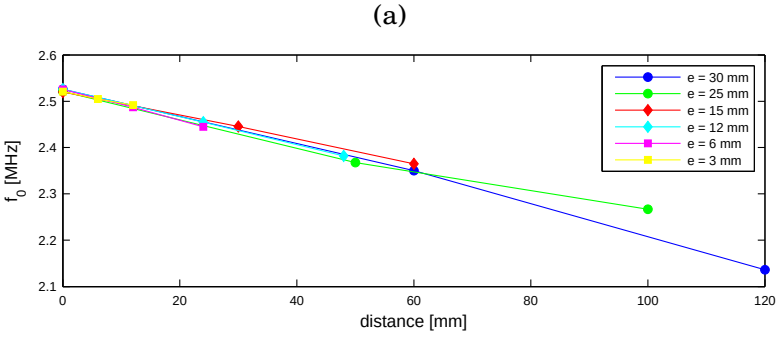

(b)

e (mm)	α_0 ($\mathrm{Np\,MHz^{-1}\,m^{-1}}$)
30	11.7
25	10.5
15	10.6
12	10.8
6	11.8
3	9.9

FIGURE 5: (a): Center frequencies of the echoes, measured from Plexiglas plates, with a transducer of center frequency 2.25 MHz. (b): Corresponding α_0 values in $\mathrm{Np\,MHz^{-1}\,m^{-1}}$.

Application of the discrete convolution model

In this part we use a data measurement performed from a 25 mm thick Plexiglas plate with a 2.25 MHz probe. We check the validity of the model presented in equation (15). The reference

waveform to build the convolution matrix $\mathbf{H}$ is assumed to be the front wall echo. It is coherent since it is the waveform unmodified by the frequency-dependent attenuation in the material. We test three models derived from equation (15):

1. without attenuation: $\mathbf{A}_1 = \mathbf{I} \Longrightarrow \boldsymbol{y}_1 = \mathbf{H}\,\boldsymbol{x}$
2. with the Olofsson's attenuation: parameter $a \Longrightarrow \boldsymbol{y}_2 = \mathbf{H}\,\mathbf{A}_2\,\boldsymbol{x}$
3. with linear attenuation: parameter $\alpha_0 \Longrightarrow \boldsymbol{y}_3 = \mathbf{H}\,\mathbf{A}_3\,\boldsymbol{x}$

The parameter a of the Olofsson's model is empirically set in order to give the lowest residue between the model and the data. α_0 is set to the mean value found in the previous part. Time positions and amplitudes are estimated by a matched filter method, taking the three models presented above. It can be seen as a simple deconvolution technique finding the better single shape in a least squares sense [1].

The data estimations through the discrete models are illustrated in figure (6). We focus on the two first back-wall echoes. The residue between the data and the model is then computed to observe the error. Globally, we can see that including the attenuation in the model achieves a better data-fitting. In particular, the linear attenuation model is close to the real waveform shapes and is consequently better adapted here. It tends to validate the linear attenuation model, that we observed in the previous part, for this particular material.

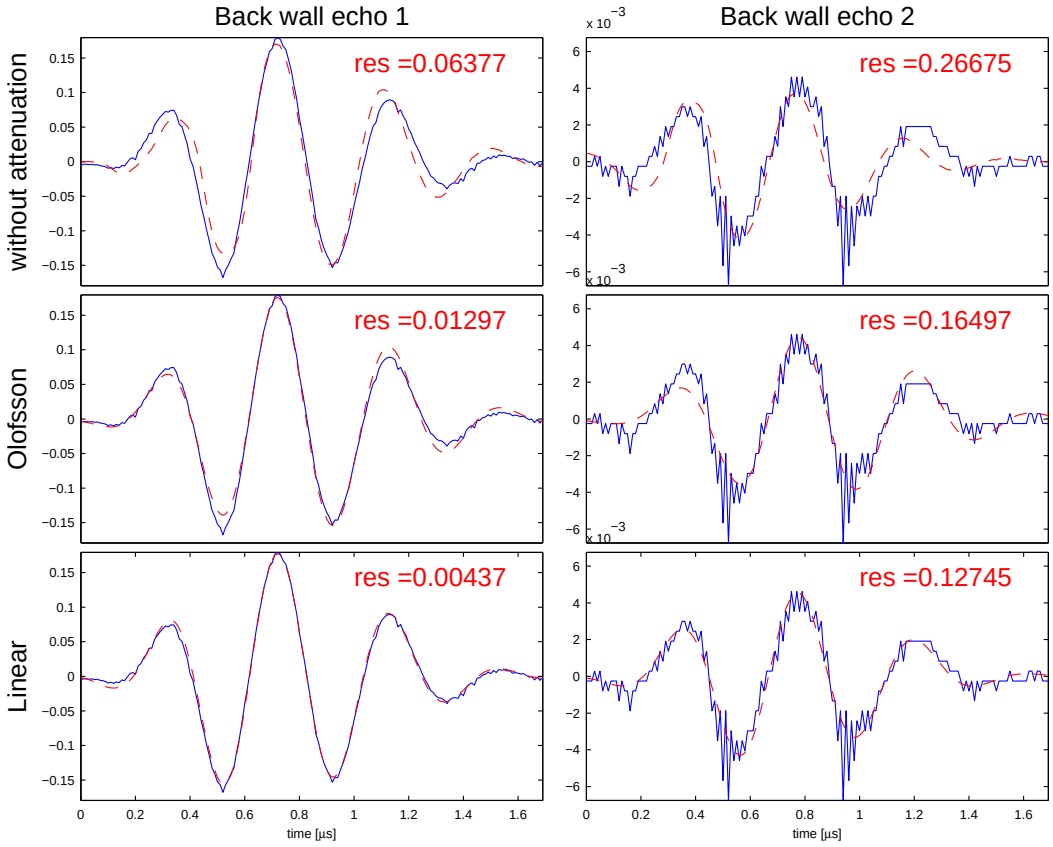

FIGURE 6: Model validity of two backwall echoes, without attenuation, with the Olofsson's model and with the linear attenuation model. '–': data, '- -': model.

CONCLUSION

Considering the propagation of ultrasonic waves through an attenuative medium, we have detailed the formation of a signal received by an ultrasonic transducer. The specific case of log-linear attenuation is equivalent to the well-known constant-Q model, highly employed in the geophysics community. It leads to the loss of high frequencies with propagation distance. From this continuous time model, we derived a discrete model employed for real data processing. After a certain propagation

distance, the attenuation impulse response corresponds to several self-convolutions of a unique attenuation kernel. The latter models the transfer function between two sampling depths, related to the sampling frequency. We described two kernel models. The first proposed by Olofsson uses a simple, first order kernel, and the second uses the linear attenuation model. Experimental data acquired from Plexiglas plates enabled us to identify the parameter of linear attenuation. Furthermore, data models were compared to real data, showing the accuracy of including linear attenuation in the discrete model. These results promise improvements for the deconvolution of complex ultrasonic data, due to a better data-fitting. This study has to be pursued to check other complex materials and other attenuation models. The model can also be improved by including a dispersion term.

ACKNOWLEDGMENT

This work has been partially supported by the French Region *Pays de la Loire* as part of the scientific program "Non-Destructive Testing and Evaluation-Pays de la Loire" (ECND-PdL).

REFERENCES

[1] S.-K. Sin and C.-H. Chen, “A comparison of deconvolution techniques for the ultrasonic nondestructive evaluation of materials”, IEEE Transactions on Image Processing **1**, 3–10 (1992).

[2] M. S. O’Brien, A. N. Sinclair, and S. M. Kramer, “Recovery of a sparse spike time series by L1 norm deconvolution”, IEEE Transactions on Signal Processing **42**, 3353–3365 (1994).

[3] T. Olofsson and T. Stepinski, “Minimum entropy deconvolution of pulse-echo signals acquired from attenuative layered media”, The Journal of the Acoustical Society of America **109**, 2831–2839 (2001).

[4] R. Kuc, M. Schwartz, and L. Micsky, “Parametric estimation of the acoustic attenuation coefficient slope for soft tissue”, in *Ultrasonics Symposium*, 44–47 (1976).

[5] A. C. Kak and K. A. Dines, “Signal processing of broadband pulsed ultrasound: Measurement of attenuation of soft biological tissues”, IEEE Transactions on Biomedical Engineering **BME-25**, 321–344 (1978).

[6] P. A. Narayana and J. Ophir, “A closed form method for the measurement of attenuationin nonlinearly dispersive media”, Ultrasonic Imaging **5**, 117–21 (1983).

[7] E. Kjartansson, “Constant Q-Wave Propagation and Attenuation”, Journal of Geophysical Research **84**, 4737–4748 (1979).

[8] D. Hale, “An inverse Q-filter”, Technical Report, Stanford Exploration Project (1981).

[9] M. Fink and J.-F. Cardoso, “Diffraction effects in pulse-echo measurement”, IEEE Transactions on Sonics and Ultrasonics **31**, 313–329 (1984).

[10] P. R. Stephanishen, “Transient radiation from pistons in an infinite baffle”, The Journal of American Society of America **49**, 1629–1638 (1971).

[11] M. O’Donnell, E. T. Jaynes, and J. G. Miller, “General relationships between ultrasonic attenuation and dispersion”, The Journal of the Acoustical Society of America **63**, 1935–1937 (1978).

[12] K. Wear, “The effects of frequency-dependent attenuation and dispersion on sound speed measurements: applications in human trabecular bone”, IEEE Transactions on Ultrasonics, Ferroelectrics and Frequency Control **47**, 265–273 (2000).